THE OFFICIAL MAGAZINE OF THE OCEANOGRAPHY SOCIETY

Oceanography

CITATION

Romeiser, R. 2013. The future of SAR-based oceanography: High-resolution current measurements by along-track interferometry. *Oceanography* 26(2):92–99, http://dx.doi.org/10.5670/oceanog.2013.37.

DOI

http://dx.doi.org/10.5670/oceanog.2013.37

THE FUTURE OF SAR-BASED OCEANOGRAPHY

High-Resolution Current Measurements by Along-Track Interferometry

BY ROLAND ROMEISER

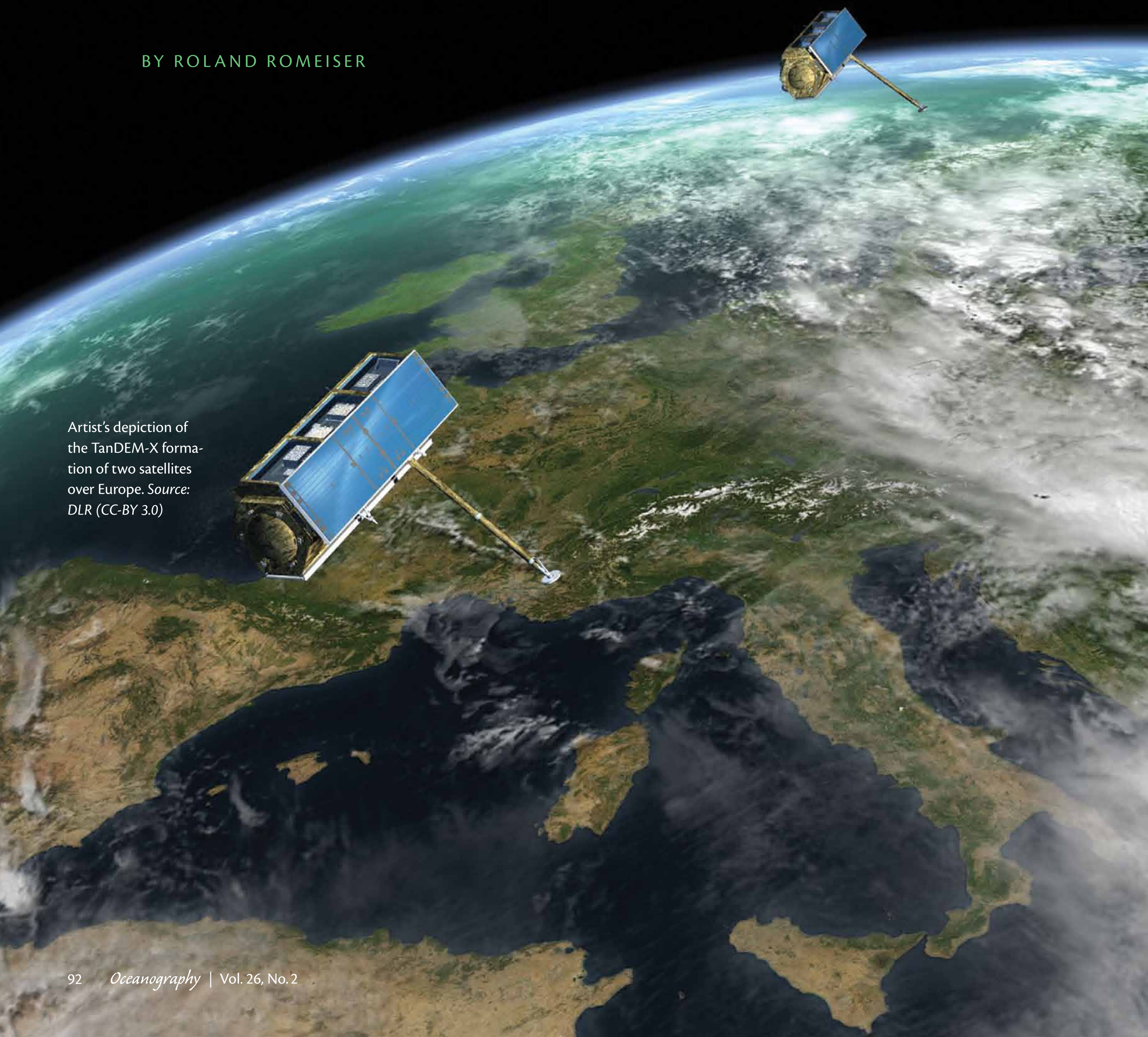

Artist's depiction of the TanDEM-X formation of two satellites over Europe. *Source: DLR (CC-BY 3.0)*

ABSTRACT. Since the Seasat mission in 1978, an impressive amount of information on oceanic and atmospheric features over the ocean has been derived from the thousands of images provided by spaceborne synthetic aperture radars (SARs). One important quantity that cannot be derived easily from conventional SAR data is the velocity of objects—current features and waves are visible in SAR intensity images because they modulate ocean surface roughness and slope, not because of direct sensitivity to their motions. Because of this indirect imaging mechanism, the quantitative interpretation of SAR signatures of spatially varying currents is challenging, and absolute current velocity retrievals are not possible at all. This situation can be improved by implementing operational along-track interferometry (ATI) capabilities on future SAR satellites. The ATI technique permits direct velocity measurements with spatial resolutions on the order of 100 m, which would be attractive for many applications. The ATI concept was developed more than 25 years ago, and its potential has been demonstrated in a number of experiments with airborne and spaceborne systems. This article provides an overview of the state of the art, promising applications, and expected further developments.

INTRODUCTION

Radar signals scattered by moving objects experience a Doppler shift in frequency, which can be exploited to measure their speeds. Synthetic aperture radars (SARs) record the Doppler spectrum of received signals, but the special data processing that enables the high spatial resolution of SAR images, called "aperture synthesis," is based on the assumption that all Doppler shifts are due to the relative motion between the radar platform (satellite or aircraft) and scatterers that are at rest on the ground plane. As a result, processed full-resolution SAR images do not contain Doppler information that would permit direct velocity estimates for individual pixels for ocean surface current or wave motion retrievals.

Traditionally, information on current features and waves has been derived from SAR image intensity variations. Ocean waves become visible in SAR images because of their periodic modulation of the local incidence angle and surface roughness as well as a SAR-specific imaging artifact called velocity bunching. This is relatively well understood, and robust techniques for deriving wave information from SAR images have been developed. Similarly, convergent and divergent regions in the surface current field modulate short-scale surface roughness in such a way that pronounced bright and dark signatures, respectively, can become visible in a SAR image. As an example, Figure 1 shows signatures of underwater sand dunes off the coast of China in an ERS-1 SAR image. Other current features whose signatures are frequently observed in SAR images are oceanic internal waves and fronts (see Jackson et al., 2013, in this issue). While many of these signatures are very clear and as nice-looking as those in Figure 1, their quantitative interpretation in terms of current gradients can be very difficult, and absolute current velocity retrievals are not possible at all. Calkoen et al. (2001) proposed a procedure for estimating bathymetric maps by a combined analysis of SAR images and echosoundings.

Chapron et al. (2005) pioneered current retrievals from SAR data by Doppler centroid analysis. With this approach, differences between observed mean Doppler frequencies (Doppler centroids) and nominal values corresponding to the relative speed between satellite and rotating Earth in radar look direction are interpreted to be the effect of surface currents and mean contributions of wave motions. Within the last few years, others have demonstrated the soundness of this approach for a variety of test sites and SAR data from different satellites (mostly Envisat [e.g., Hansen et al., 2011] and TerraSAR-X [e.g., Romeiser et al., 2013]). Because the method does not require any special data recording, it can be applied to newly acquired SAR data sets as well as archived ones. A drawback is that the extra Doppler information is obtained at fairly low spatial resolution, usually on the order of kilometers, because Doppler centroids need to be estimated from raw data amounts corresponding to clusters of hundreds to

Roland Romeiser *(rromeiser@rsmas.miami.edu) is Associate Professor, Rosenstiel School of Marine and Atmospheric Science, University of Miami, Miami, FL, USA.*

Figure 1. ERS-1 synthetic aperture radar (SAR) image of the Xinchuan Gang Shoals along the east coast of China, north of Shanghai, acquired on July 8, 1995, 02:34 UTC. Area size = 100 km × 100 km. The signatures in the upper right half of the image result from modulation of tidal currents and surface roughness by underwater topography. *Source: European Space Agency (ESA)*

thousands of full-resolution pixels.

More than 25 years ago, Goldstein and Zebker (1987) presented the concept of SAR along-track interferometry (ATI), which permits velocity measurements at full SAR resolution. To achieve this, an ATI system uses two antennas that are separated by some distance in flight direction and that receive the same backscattered signals from the ocean or land surface with a small time lag on the order of milliseconds. After processing the data from each antenna into a full-resolution SAR image and keeping track of amplitude and phase of the signals mapped into each pixel, combined interferometric processing of the two images reveals phase differences whose expectation values can be shown to be proportional to Doppler frequencies and thus to line-of-sight scatterer velocities.

ATI ACHIEVEMENTS AND STATE OF THE ART

Goldstein and Zebker (1987) explained the basic concept of ATI and presented example results from a first experiment with an airborne system. A more systematic experiment was carried out over ship-generated internal waves at Loch Linnhe (Scotland) in 1989. A comparison between ATI-derived velocities (called "Doppler velocities" if no further corrections have been applied) and surface currents measured by in situ instrumentation revealed significant differences. Thompson and Jensen (1993) explained this discrepancy as the effect of mean contributions of subresolution-scale wave motions to the ATI signatures. Romeiser and Thompson (2000) proposed a simplified numerical model for the computation of the wave-induced contributions to Doppler velocities; Romeiser (2005) demonstrated an automatized iterative correction of data from an airborne ATI experiment for the spatially varying wave contributions that can occur as a result of hydrodynamic wave-current interaction. The numerical Doppler models use parameterizations of the wave spectrum that depend on the wind vector relative to the radar look direction, so the wind speed and direction in the test area must be known in order to do the computations. It is possible to estimate the wind field from the radar image itself. Furthermore, it has to be taken into account that the standard wave parameterizations may be inappropriate where the local wave field is not at equilibrium with the wind, which may be the case, for example, in coastal areas with strong swell waves propagating towards the coast or in rivers. The resulting current field is always supposed to be the surface current field, and it may include contributions of wind drift and Stokes drift.

In February 2000, Space Shuttle *Endeavour* became the platform of the first spaceborne SAR system with ATI capability. For the joint USA-German-Italian Shuttle Radar Topography Mission (SRTM), the *Endeavour* was equipped with antennas in the cargo bay and on the end of a 60 m long antenna boom. Optimized for topography measurements over land, the antenna boom was oriented perpendicular to the flight direction to create a long cross-track "baseline" between the antennas. An additional effective along-track baseline of 3.5 m that occurred for mechanical reasons was sufficient to demonstrate current measurements over the Dutch Wadden Sea (Romeiser et al., 2005) and over the Elbe River, Germany (Romeiser et al., 2007). Figure 2 shows the result obtained for the Wadden Sea, together with a corresponding reference current field from the numerical circulation model KUSTWAD. Due to suboptimal system parameters, the interferogram had to be averaged over many pixels to reduce phase noise. The effective spatial resolution of the resulting SRTM-derived line-of-sight current field was found to be on the order of 1 km, with a remaining rms uncertainty for the currents of about 0.1 m s^{-1}. Aside from the relatively low resolution, the qualitative and quantitative agreement between the SRTM- and model-derived current fields was found to be good and consistent with theoretical expectations. Similar results were obtained for the Elbe River case.

Romeiser and Runge (2007) studied the theoretical ATI performance of the German satellite TerraSAR-X, which has experimental divided-antenna modes of operation that permit ATI with very short effective baselines on the order of 1 m. ATI data quality similar to that of SRTM was predicted, again due to a requirement to average over many pixels for noise reduction. (Compared to SRTM, a larger number of TerraSAR-X pixels need to be averaged to obtain the same data quality, due to a shorter baseline and a higher instrument noise level, but, at the same time, the TerraSAR-X pixels are much smaller.) Further numerical simulation results indicated that effective spatial resolutions of 100 m and better could be obtained with a longer along-track distance between the antennas and a reduced instrument noise level. The quoted effective resolutions are understood to be those that reach a remaining rms uncertainty of 0.1 m s^{-1}. There is always a tradeoff between spatial resolution and remaining uncertainty (i.e., less spatial averaging can be used where high resolution is needed, or more averaging can be used to obtain particularly smooth current fields). However, averaging over large areas makes sense only where the current field is sufficiently homogeneous. Furthermore, uncertainties in the absolute phase calibration can

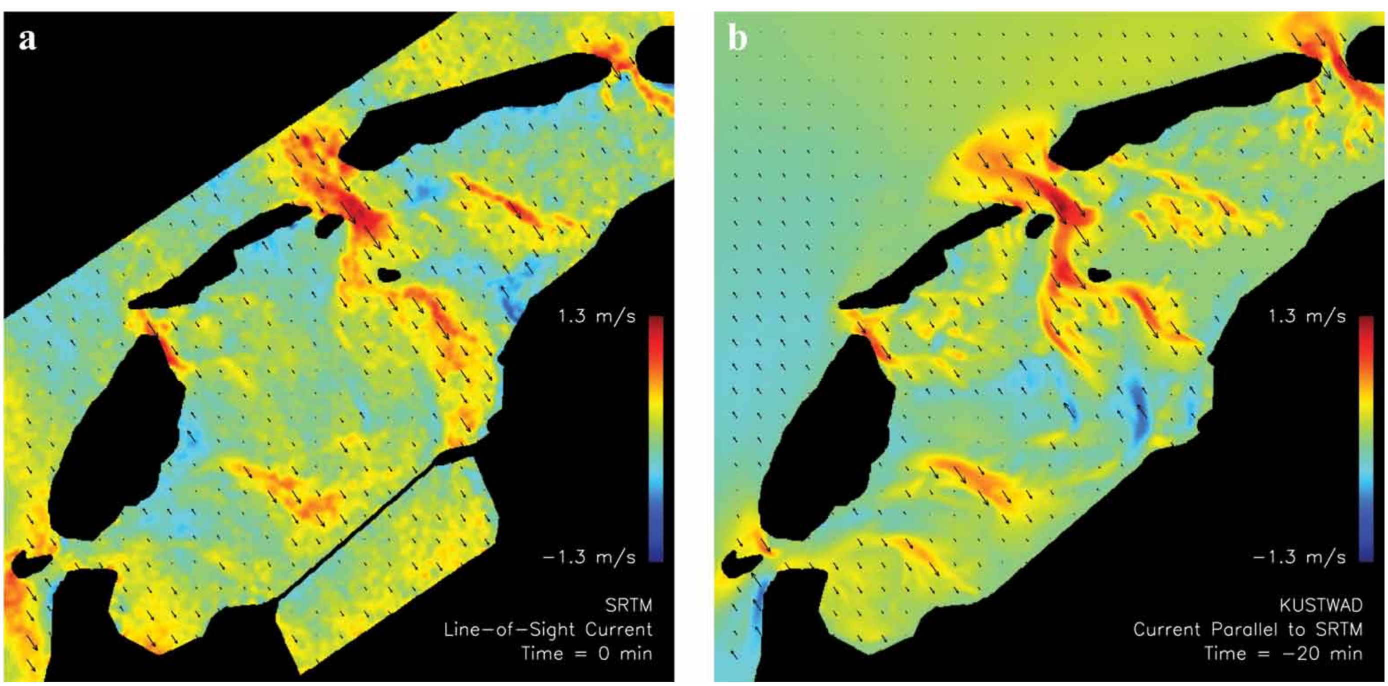

Figure 2. (a) Line-of-sight current field in the Dutch Wadden Sea derived from a Shuttle Radar Topography Mission (SRTM) image acquired on February 15, 2000, 12:34 UTC. (b) Reference current field from a numerical circulation model. Area size = 70 km × 70 km. Radar look direction = toward northwest. Flight direction = toward northeast. *From Romeiser et al. (2005)*

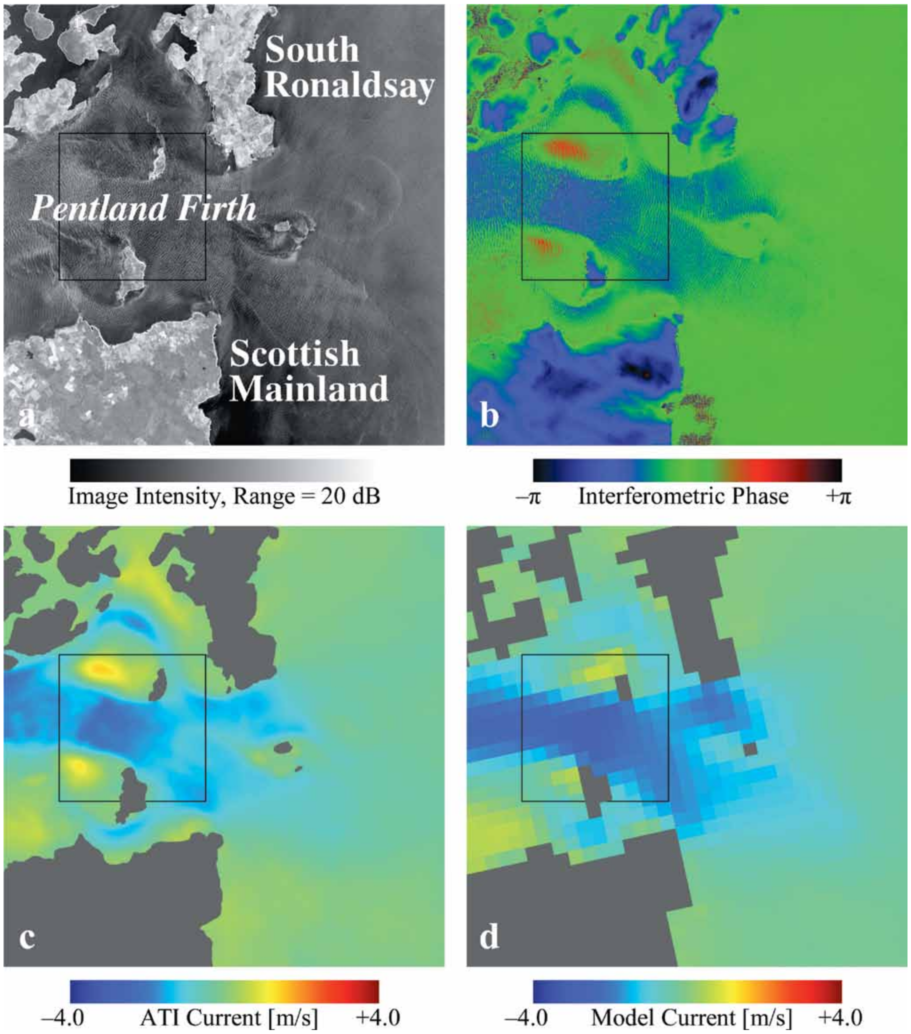

Figure 3. TanDEM-X data acquired over Pentland Firth (Scotland) on February 26, 2012, 06:41 UTC. (a) Radar intensity image. (b) Interferometric phase image. (c) Derived line-of-sight current field. (d) Reference current field from a numerical tide computation system. Area size = 30 km × 30 km. Radar look direction = from right to left. Positive flow direction = from left to right. Flight direction = from top to bottom. The black frame outlines the area of the subimage presented in Figure 4.

cause bias in retrieved velocities that cannot be reduced by averaging.

According to Romeiser and Runge (2007), an effective along-track baseline on the order of 20–50 m, corresponding to a physical antenna distance of 40–100 m, is optimal for the best ATI data quality at X-band, the 9.6 GHz frequency band used by SRTM and TerraSAR-X. This baseline range corresponds to time lags of ~ 3–7 ms between the SAR data received by the two antennas. In general, data quality decreases when there are shorter time lags because the ATI phase becomes less sensitive to scatterer velocities, so that effects of instrument noise become more dominant. With longer time lags, data quality suffers from temporal decorrelation of the backscattered signal. The ideal time lag/along-track baseline range scales with the radar wavelength (i.e., ATI systems operating at higher frequencies need shorter along-track baselines for optimal performance).

TerraSAR-X was launched in June 2007, and the first ATI images were acquired over the Elbe River in spring and summer 2008. Romeiser et al. (2010b) analyzed these data and found good agreement with theoretical expectations (i.e., data quality similar to that of SRTM). While this was an encouraging result, the ATI performance of TerraSAR-X with its suboptimal effective baseline is not much better than what can be achieved by Doppler centroid analysis of conventional SAR data. This problem could be overcome for the first time when we had a chance to acquire a few data sets with near-optimal along-track baselines using the TanDEM-X formation of two satellites. The TanDEM-X formation consists of the original TerraSAR-X satellite and an almost-identical twin that was launched in 2010. They orbit Earth together on slightly different elliptical orbits, resulting in a helical relative motion pattern optimized for topography measurements over land by cross-track interferometry (see illustration on the first page of this article). Most of the time, their along-track distance is too long for inter-satellite interferometry over water, but special orbit parameters used during a limited period in February and March 2012 enabled us to acquire very high-quality data over selected ocean test sites, such as Pentland Firth between the Scottish mainland and the Orkney Islands, a region known for its strong tidal currents.

Figure 3 shows data acquired at this test site on February 26, 2012, with an effective along-track baseline of 25 m, and a reference current field from the numerical tide computation system POLPRED. The ATI-derived line-of-sight current field and the model result (Figure 3c,d) were found to agree well. In fact, the ATI result is believed to be more accurate than the model result, because the available version of POLPRED suffered from poor spatial resolution of 1 km and outdated bathymetry for this area. The full potential of the TanDEM-X data and of spaceborne ATI in general becomes visible in Figure 4, which shows image intensity and Doppler velocity variations in a 10 km × 10 km subsection of the test area at a higher resolution (i.e., with less smoothing) than Figure 3a and c. On spatial scales that would be dominated by phase noise in SRTM and TerraSAR-X divided-antenna mode data, the TanDEM-X data set shows clear signatures of orbital wave motions at wavelengths on the order of 200 m.

Detailed analysis indicates that the effective resolution of the TanDEM-X-derived Doppler velocities in this example is on the order of 33 m (for a residual rms velocity uncertainty of 0.1 m s^{-1}). At this quality level, ATI data are suitable for direct measurements of wave motion as well as high-resolution measurements of surface current variations over ocean fronts or internal waves or in narrow rivers. Romeiser et al. (2013) present a complete analysis of this TanDEM-X data set and another one acquired 22 days later with an effective baseline of 40 m.

So far, all spaceborne SAR systems with ATI capabilities have been limited to one-dimensional measurements of the line-of-sight component of scatterer velocities. Toporkov et al. (2005) demonstrated with an experimental airborne ATI system that this can be changed if two pairs of antennas with different look directions relative to the platform motion are used. Combining such a setup with system parameters on a TanDEM-X-like quality level, future spaceborne ATI systems could provide fully two-dimensional vector current measurements at an effective spatial resolution better than 100 m.

EXPECTED FURTHER DEVELOPMENTS

Current measurements by ATI seem to be particularly promising for coastal-area applications that require high spatial resolution, such as bathymetric monitoring, siting of turbines for tidal energy harvesting, and other coastal engineering applications. Figure 5 shows an example of ATI-based bathymetry

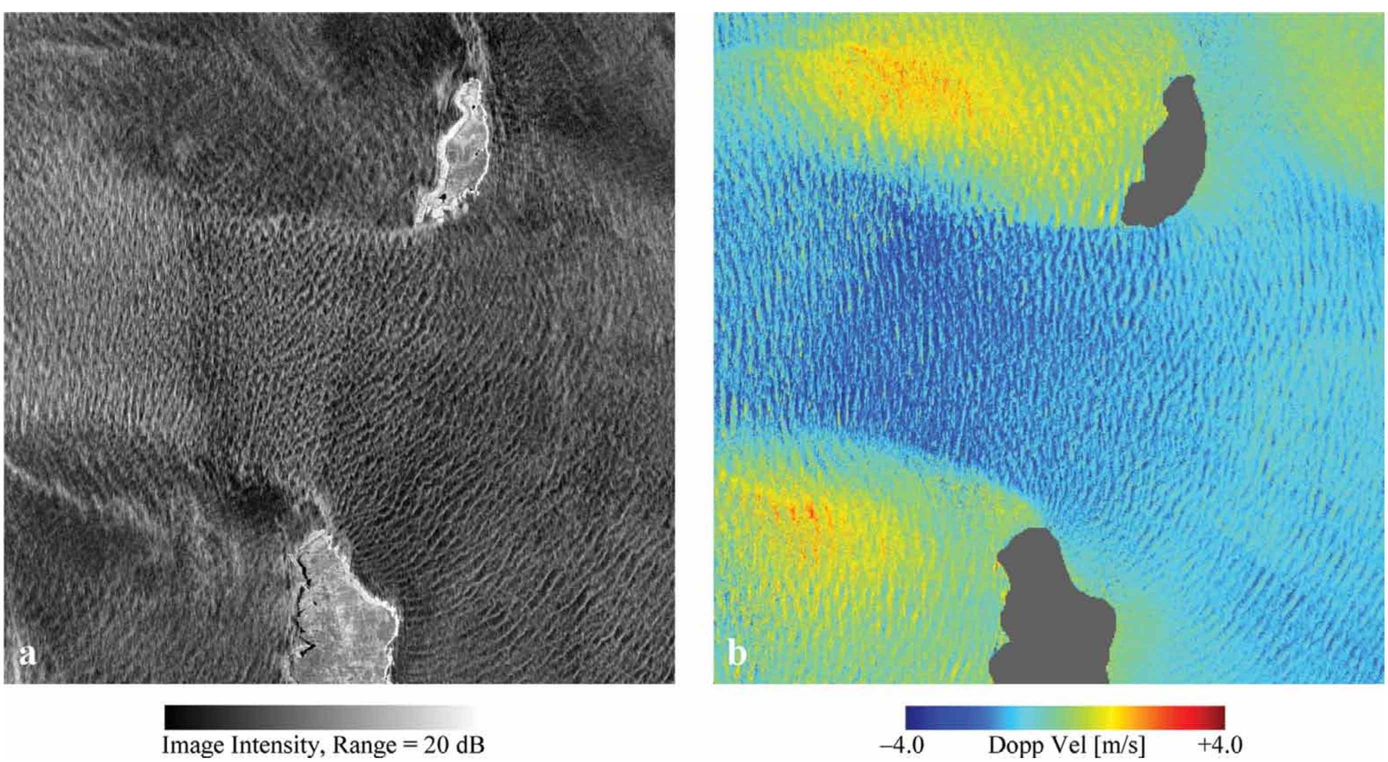

Figure 4. A 10 km × 10 km subsection of the Figure 3 data set showing signatures of surface waves in (a) the intensity image, and (b) the full-resolution Doppler velocity image derived from the interferogram.

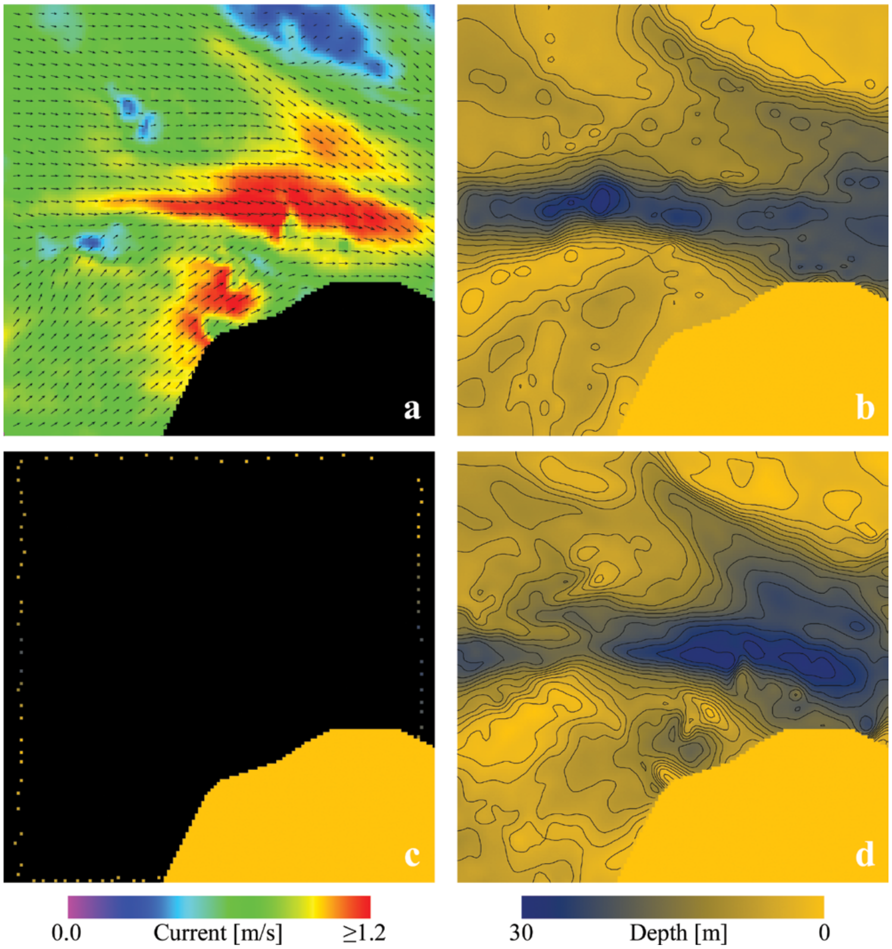

Figure 5. Bathymetry retrieval example. (a) Airborne ATI-derived vector current field north of the German island of Sylt, from an experiment in May 2001. Area size = 3.5 km × 3.5 km. Grid resolution = 25 m × 25 m. (b) Depth map from echosoundings with an effective resolution of 200 m. (c) Seventy-eight selected reference depth points near the boundaries. (d) Depth map derived from the 78 reference depths in combination with the ATI-derived current field. *From Romeiser et al. (2010a)*

retrieval. Coastal oceanographers may want to use ATI data for studies of fronts, eddies, and internal waves. Another attractive application with many potential users is the global measurement and long-term monitoring of river discharges into the ocean, as discussed by Grünler et al. (2013). In the near future, increasing interest is expected in along-track interferometry over the open ocean, where traditional remote-sensing techniques such as altimetry cannot keep up with the development of increasingly refined numerical circulation models, and there are no technological alternatives to satellite-based remote sensing. Some users may be interested in wave measurements by ATI as well, but the advantages compared to conventional SAR-based techniques seem to be less pronounced than for current measurements, as discussed by Bao et al. (1997). Romeiser et al. (2010a) discuss in more detail the potential applications of satellite-based ATI and Doppler centroid analysis and provide additional example results.

Altogether, there are plenty of scientific and commercial applications that would justify the development of a dedicated spaceborne ATI system for ocean applications. Such a system should have a near-optimal along-track baseline, which is easier to achieve at higher radar frequencies because the optimal baseline range scales with the radar wavelength (Romeiser and Thompson, 2000; Romeiser and Runge, 2007). Furthermore, it should be a dual-beam ATI system with vector current measuring capability, and it should have an accessible incidence angle range, swath width (possibly left- and right-looking at the same time), and duty cycle that enable it to access and cover large areas of the ocean with short lead and repeat times. The European Space Agency has sponsored several studies on the design of such a system in recent years (e.g., Márquez et al., 2010). The chances that we will see a dedicated ATI system for ocean applications in space within the next 10–20 years seem to be good.

ACKNOWLEDGEMENTS

Significant contributions to the work presented in this paper were made by Donald R. Thompson of The Johns Hopkins University/Applied Physics Laboratory, Laurel, MD, USA, and by Hartmut Runge, Steffen Suchandt, Ralph Kahle, Helko Breit, and Michael Eineder of the German Aerospace Center, Oberpfaffenhofen, Germany. Model current fields were provided by Karin de Jong and Jur Vogelzang of Rijkswaterstaat, The Hague/Delft, Netherlands; Norbert Winkel of the Federal Waterways Engineering and Research Institute, Hamburg, Germany; and Paul Bell of the National Oceanography

Center, Liverpool, UK. TanDEM-X data were obtained through TanDEM-X science project ATI-OCEA0599 (PI: Hartmut Runge). Roland Romeiser has been funded by the US Office of Naval Research (ONR) under grant N00014-11-1-0280 (*SARprises*).

REFERENCES

Bao, M., C. Bruening, and W. Alpers. 1997. Simulation of ocean waves imaging by an along-track interferometric synthetic aperture radar. *IEEE Transactions on Geoscience and Remote Sensing* 35:618–631, http://dx.doi.org/10.1109/36.581977.

Calkoen, C.J., G.H.F.M. Hesselmans, G.J. Wensink, and J. Vogelzang. 2001. The Bathymetry Assessment System: Efficient depth mapping in shallow seas using radar images. *International Journal of Remote Sensing* 22:2,973–2,998, http://dx.doi.org/10.1080/01431160116928.

Chapron, B., F. Collard, and F. Ardhuin. 2005. Direct measurements of ocean surface velocity from space: Interpretation and validation. *Journal of Geophysical Research* 110, C07008, http://dx.doi.org/10.1029/2004JC002809.

Goldstein, R.M., and H.A. Zebker. 1987. Interferometric radar measurement of ocean surface currents. *Nature* 328:707–709.

Grünler, S., R. Romeiser, and D. Stammer. 2013. Estimation of tidally influenced estuarine discharge from space using along-track InSAR technology: A model-based feasibility study. *Journal of Geophysical Research* 118:3,679–3,693, http://dx.doi.org/10.1002/jgrc.20269.

Hansen, M.W., J.A. Johannessen, K.F. Dagestad, F. Collard, and B. Chapron. 2011. Monitoring the surface inflow of Atlantic Water to the Norwegian Sea using Envisat ASAR. *Journal of Geophysical Research* 116, C12008, http://dx.doi.org/10.1029/2011JC007375.

Jackson, C.R., J.C.B. da Silva, G. Jeans, W. Alpers, and M.J. Caruso. 2013. Nonlinear internal waves in synthetic aperture radar. *Oceanography* 26(2):68–79, http://dx.doi.org/10.5670/oceanog.2013.32.

Márquez, J., G. Ruffini, D. Lancashire, B. Richards, and C. Buck. 2010. Wavemill: A novel instrument for ocean circulation monitoring. Pp. 52–54 in *Proceedings of EUSAR 2010, June 7–10, 2010*. Eurogress, Aachen, Germany, VDE Verlag.

Romeiser, R. 2005. Current measurements by airborne along-track InSAR: Measuring technique and experimental results. *IEEE Journal of Oceanic Engineering* 30:552–569, http://dx.doi.org/10.1109/JOE.2005.857508.

Romeiser, R., H. Breit, M. Eineder, H. Runge, P. Flament, K. de Jong, and J. Vogelzang. 2005. Current measurements by SAR along-track interferometry from a space shuttle. *IEEE Transactions on Geoscience and Remote Sensing* 43:2,315–2,324, http://dx.doi.org/10.1109/TGRS.2005.856116.

Romeiser, R., J. Johannessen, B. Chapron, F. Collard, V. Kudryavtsev, H. Runge, and S. Suchandt. 2010a. Direct surface current field imaging from space by along-track InSAR and conventional SAR. Pp. 73–91 in *Oceanography From Space, Revisited*. V. Barale, J.F.R. Gower, and L. Alberotanza, eds, Springer Science+Business Media.

Romeiser, R., and H. Runge. 2007. Theoretical evaluation of several possible along-track InSAR modes of TerraSAR-X for ocean current measurements. *IEEE Transactions on Geoscience and Remote Sensing* 45:21–35, http://dx.doi.org/10.1109/TGRS.2006.885405.

Romeiser, R., H. Runge, S. Suchandt, R. Kahle, C. Rossi, and P.S. Bell. 2013. Quality assessment of surface current fields from TerraSAR-X and TanDEM-X along-track interferometry and Doppler centroid analysis. *IEEE Transactions on Geoscience and Remote Sensing* PP(99):1–14, http://dx.doi.org/10.1109/TGRS.2013.2265659.

Romeiser, R., H. Runge, S. Suchandt, J. Sprenger, H. Weilbeer, A. Sohrmann, and D. Stammer. 2007. Current measurements in rivers by spaceborne along-track InSAR. *IEEE Transactions on Geoscience and Remote Sensing* 45:4,019–4,030, http://dx.doi.org/10.1109/TGRS.2007.904837.

Romeiser, R., S. Suchandt, H. Runge, U. Steinbrecher, and S. Grünler. 2010b. First analysis of TerraSAR-X along-track InSAR-derived current fields. *IEEE Transactions on Geoscience and Remote Sensing* 48:820–829, http://dx.doi.org/10.1109/TGRS.2009.2030885.

Romeiser, R., and D.R. Thompson. 2000. Numerical study on the along-track interferometric radar imaging mechanism of oceanic surface currents. *IEEE Transactions on Geoscience and Remote Sensing* 38:446–458, http://dx.doi.org/10.1109/36.823940.

Thompson, D.R., and J.R. Jensen. 1993. Synthetic aperture radar interferometry applied to ship-generated waves in the 1989 Loch Linnhe experiment. *Journal of Geophysical Research* 98:10,259–10,269, http://dx.doi.org/10.1029/93JC00429.

Toporkov, J.V., D. Perkovic, G. Farquharson, M.A. Sletten, and S.J. Frasier. 2005. Sea surface velocity vector retrieval using dual-beam interferometry: First demonstration. *IEEE Transactions on Geoscience and Remote Sensing* 43:2,494–2,502, http://dx.doi.org/10.1109/TGRS.2005.848603.